

Modular Coupling of Iron Nanozyme and Natural Enzyme in Responsive Microgel Reactors for Enhanced Cascade Catalysis

Divya Gaur and Bijay P. Tripathi*

Functional Materials & Membranes Laboratory, Department of Materials Science & Engineering, Indian Institute of Technology Delhi, New Delhi, 110016, India

Email: bptripathi@mse.iitd.ac.in; drbptripathi@gmail.com

Table of Contents

| | |
|--|----|
| S1. SUPPORTING METHODS | 2 |
| S1.1. Characterization methods | 2 |
| <i>Figure S1. FTIR spectra and ¹H NMR for monomer O-acryloyl -L-serine (AcSer)</i> | 3 |
| <i>Figure S2. EDS spectrum and elemental mapping of Fe-PNSER microgel</i> | 4 |
| <i>Figure S3. ¹H NMR spectrum for Fe₃O₄-loaded poly(N-isopropylacrylamide-co-serine) (Fe-PNSER) microgel dispersed in D₂O (500 Hz)</i> | 4 |
| <i>Figure S4. Reversible size variation of Fe-PNSER microgels in water with change in temperatures (24-50 °C). Error bars represent three replicates</i> | 5 |
| <i>Figure S5. DLS profile of Fe-PNSER microgel after sonication; Z-average = 390 nm, PDI = 0.01</i> | 6 |
| <i>Figure S6. Stability of microgelsomes. Photographic images of (A) microgelsomes dispersed in oil phase, ruptured microgelsomes (B) upon centrifugation and (C) stored at 4 °C for 12 h. FESEM images of microgelsomes (D) after centrifugation, (E) microgelsomes dispersed in water and stored for 1 month at room temperature</i> | 7 |
| <i>Figure S7. Calibration curves for FITC-dextran and enzymes glucose oxidase (GOx) and horseradish peroxidase (HRP)</i> | 7 |
| <i>Scheme S1. Schematic representation of the mechanistic pathway for the peroxidase-like activity of transition Fe₃O₄ nanoparticles.[2]</i> | 8 |
| <i>Figure S8. Lineweaver Burk plot and kinetic parameters (V_{max} and K_m) of microreactors HRP-MGC and Fe-MGC. Error bars represent three replicates</i> | 8 |
| <i>Figure S9. Enzymatic activity of free GOx and HRP at pH 3 and pH 5. Error bars represent three replicates</i> | 9 |
| <i>Table S1. Encapsulation efficiency of Fe-MGC for different encapsulants</i> | 10 |
| <i>Table S2. Specific activity (V₀) of microgelsomes microreactor for the oxidation reaction at different pH values. Error bars represent three replicates</i> | 10 |

S1. SUPPORTING METHODS

S1.1. Characterization methods

Transmission electron microscopy (TEM) analysis was performed on a JEOL-1400 TEM to analyze the internal morphology and particle size of the PNSER core-shell microgel particles. The microgel samples were prepared using drop-casting method. Aqueous dispersion of microgel (0.001 mg/ mL) was drop-casted onto a carbon-coated copper grid and dried at room temperature for 24 h in anhydrous condition.

Field emission scanning electron microscopy was performed to study the surface morphology and topography of the microgels and PNSER microgels-derived microgelsomes using (FE-SEM, JSM-7800F Prime, JEOL instrument. The aqueous dispersion of samples was drop-casted on a clean glass slide and air-dried under anhydrous conditions. The specimens were sputter coated with 10 nm platinum and characterized at 5kV accelerating voltage.

Atomic force microscopy (AFM) images of microgels were performed on a Bruker Multimode instrument with a Quadrex Nanoscope 3D controller. Samples were drop-casted onto a silica wafer and air-dried overnight.

Confocal laser scanning microscopy (CLSM) was performed to analyse the microgelsomes formation, their particle size, stability and encapsulation of guest molecules using Leica Microsystems, Germany at 100x magnifications. Samples were prepared by adding a 5 μ L dispersion of freshly prepared microgelsomes on a clean glass slide and covered with a glass coverslip for microscopic analysis.

X-ray diffraction (XRD) The crystallographic structure of Ag NPs in microgel was analysed using Bruker D8 advance X-ray diffractor.

Thermogravimetric analysis (TGA) of microgels was performed under inert conditions from RT to 700 °C, ramp rate 5 °C min⁻¹, using SDT-Q600, thermogravimetric analyser (TA Instruments, France).

Dynamic light scattering was used to characterize the microgel particle size in water and 2-ethyl-1-hexanol with response to temperature and their surface charge behavior with respect to pH was measured on a Zeta sizer Ver. 7.11., Malvern Instruments, UK.

Interfacial tension between the microgel-rich aqueous phase and 2-ethyl 1-hexanol was measured using du Noüy ring method on a manual tensiometer (Testing instruments S1 manufacturing company). The aqueous microgel dispersion was filled in a glass apparatus, and du Noüy ring was immersed 4mm below the surface, followed by the careful addition of 2-ethyl 1-hexanol. The du Noüy ring was then slowly lifted upwards until the lamella tore off the ring and the interfacial tension was measured.

S1.2 Labelling of enzymes with fluorescent dyes

To validate the encapsulation of enzymes in microgelsomes, the enzymes glucose oxidase (GOx) and hydrogen peroxide (HRP) were labeled with a fluorescent dye, fluorescein isothiocyanate (FITC), and rhodamine B isothiocyanate (RITC), respectively. Typically, enzymes (5 mg) were dissolved in 2 mL sodium carbonate buffer (pH 8.5, 100 mM), followed by the dropwise addition of 50 μ L of fluorescein isothiocyanate (FITC) or rhodamine B isothiocyanate (RITC) dissolved in DMSO solution (1 mg/mL). The solution was stirred at 0 $^{\circ}$ C for 5 h and purified using an amplicon dialysis tube (10 kDa) via centrifugation, which was then freeze-dried and stored at -20 $^{\circ}$ C for further use.[1]

S1.3 Labeling microgel particles with fluorescent dye

Fe-PNSER microgels (20 mg) were dispersed in 2 mL sodium bicarbonate buffer (pH 8.5, 100 mM). A 50 μ L of FITC DMSO solution (1 mg/mL) was added dropwise and the dispersion was stirred at 15 $^{\circ}$ C for 5 h. The unbound dye molecules were removed by repeated centrifugation at 15000 rpm for 10 min and freeze-dried.

S1.4 Staining oil with fluorescent dye

For the CLSM analysis of O/W emulsion, 2-ethyl 1-hexanol was mixed with 5 μ L hydrophobic dye Nile Red.

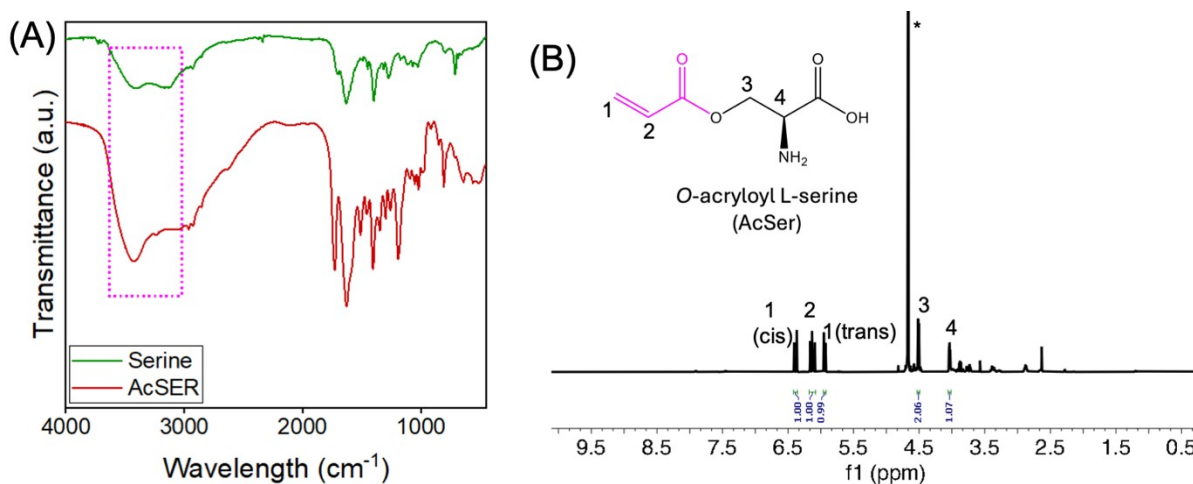


Figure S1. FTIR spectra and ^1H NMR for monomer *O*-acryloyl -L-serine (AcSer).

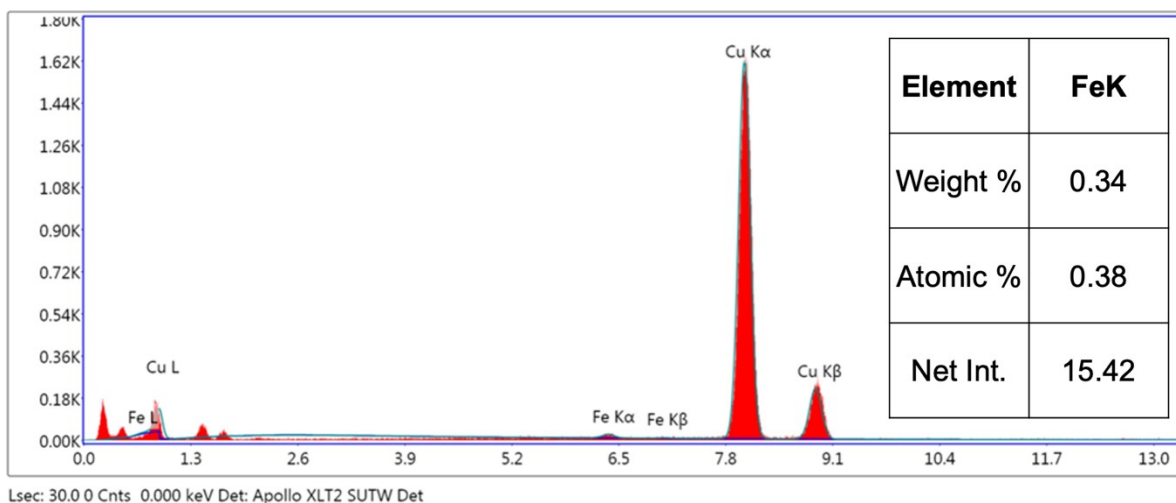


Figure S2. EDS spectrum and elemental mapping of Fe-PNSER microgel.

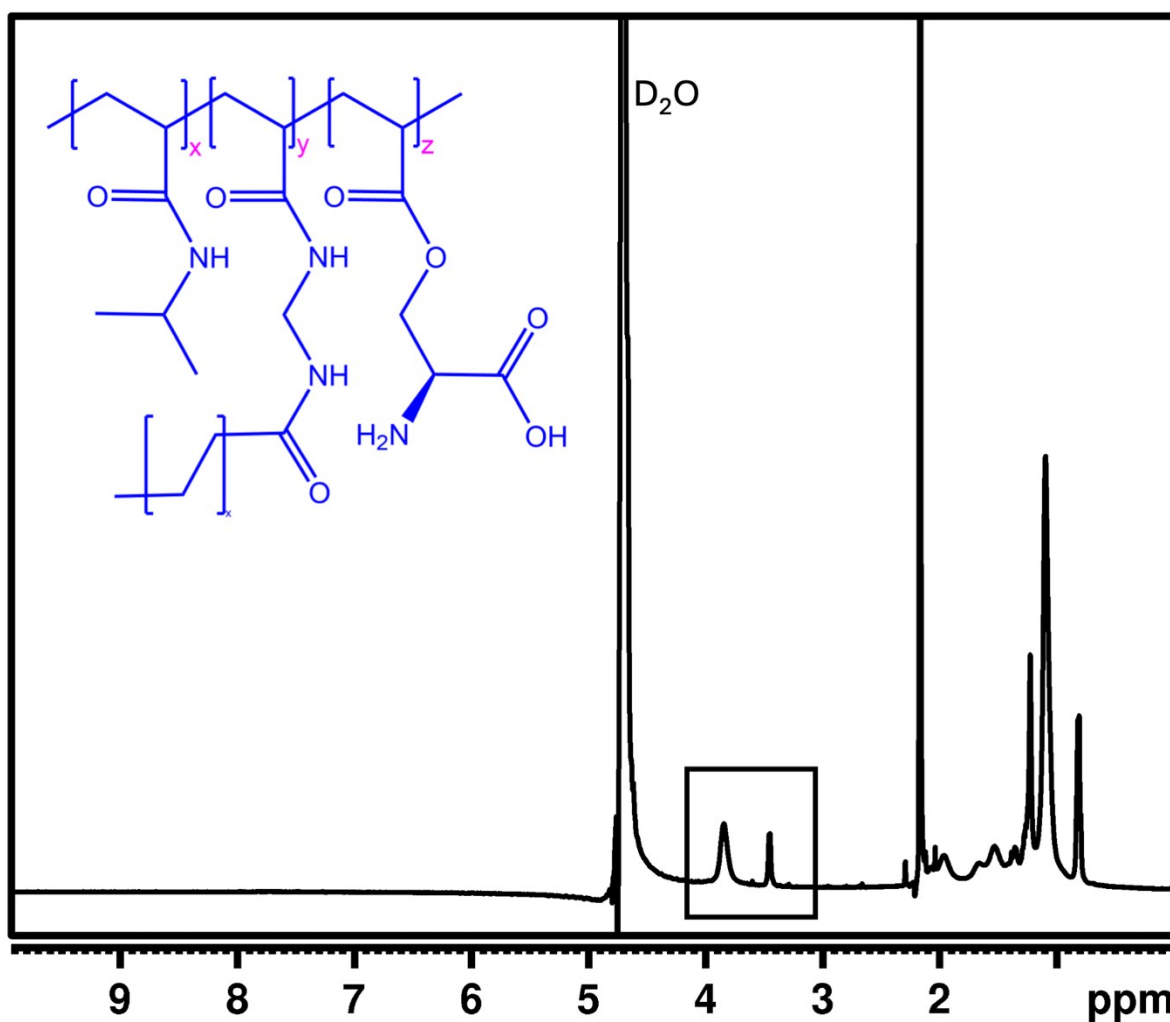


Figure S3. 1H NMR spectrum for Fe_3O_4 -loaded poly(N-isopropylacrylamide-co-serine) (Fe-PNSER) microgel dispersed in D_2O (500 Hz).

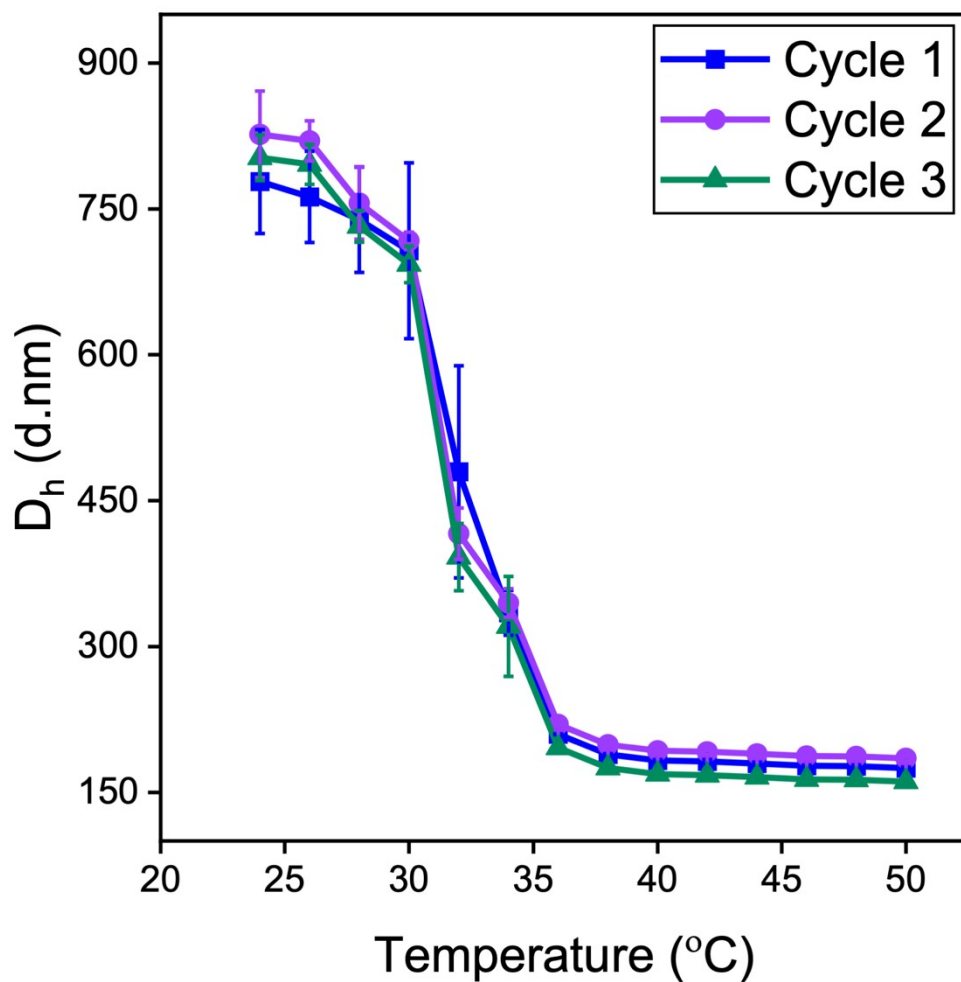


Figure S4. Reversible size variation of Fe-PNSER microgels in water with change in temperatures (24-50 $^{\circ}\text{C}$). Error bars represent three replicates.

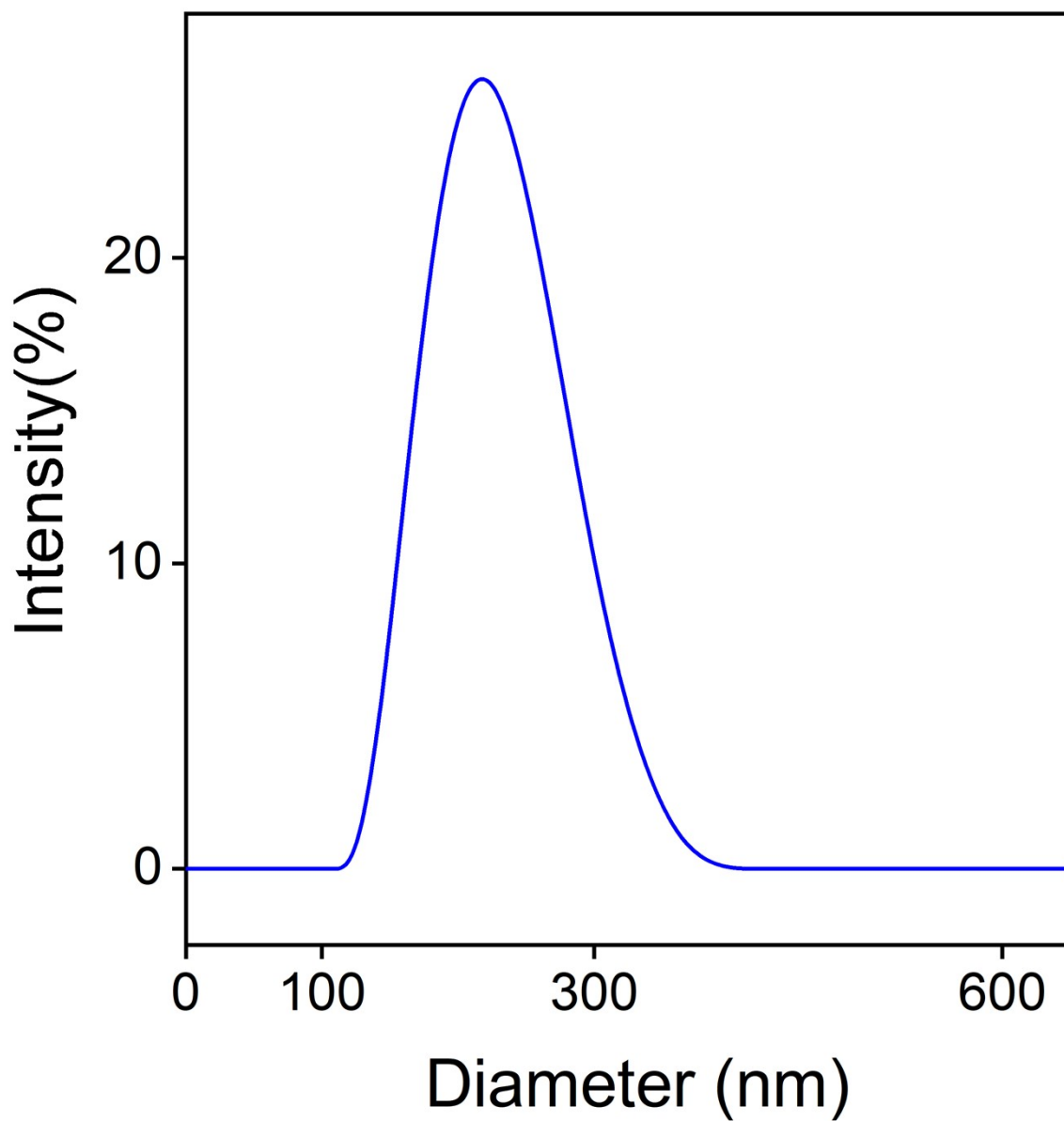


Figure S5. DLS profile of Fe-PNSER microgel after sonication; Z-average = 390 nm, PDI = 0.01.

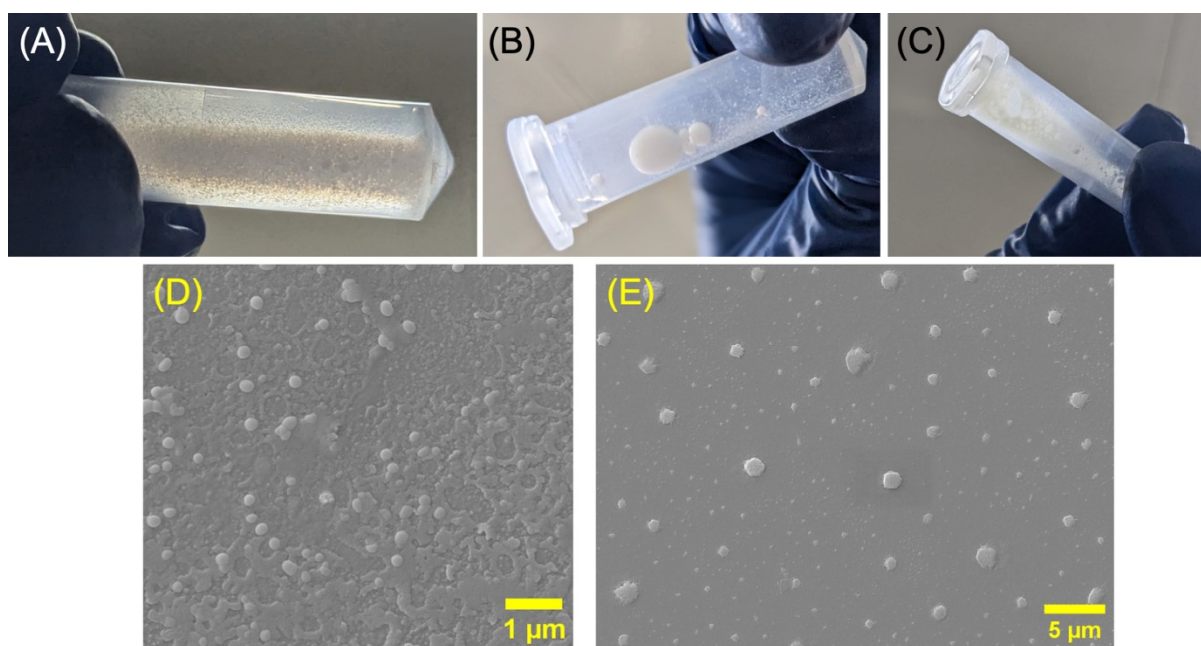


Figure S6. Stability of microgelsomes. Photographic images of (A) microgelsomes dispersed in oil phase, ruptured microgelsomes (B) upon centrifugation and (C) stored at 4 °C for 12 h. FESEM images of microgelsomes (D) after centrifugation, (E) microgelsomes dispersed in water and stored for 1 month at room temperature.

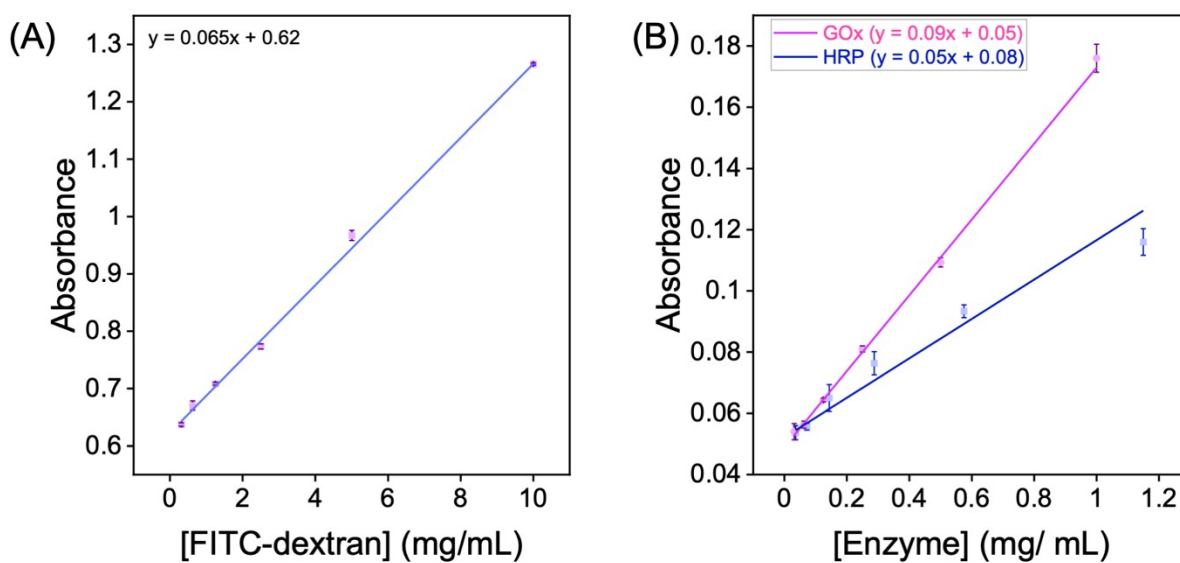
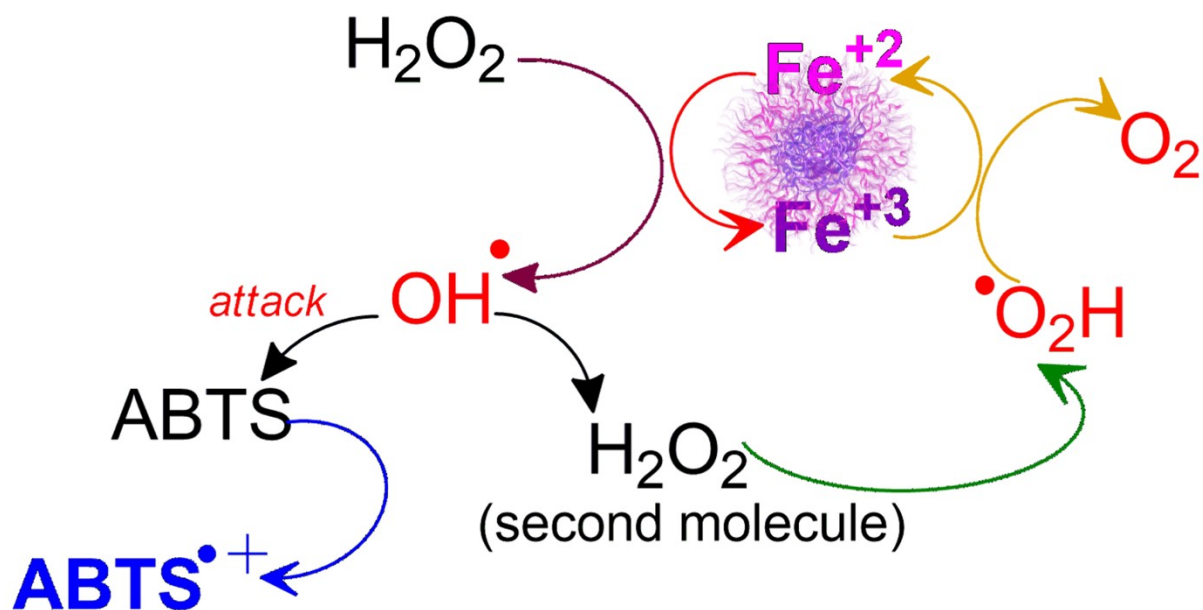


Figure S7. Calibration curves for FITC-dextran and enzymes glucose oxidase (GOx) and horseradish peroxidase (HRP).



Scheme S1. Schematic representation of the mechanistic pathway for the peroxidase-like activity of transition Fe₃O₄ nanoparticles.[2]

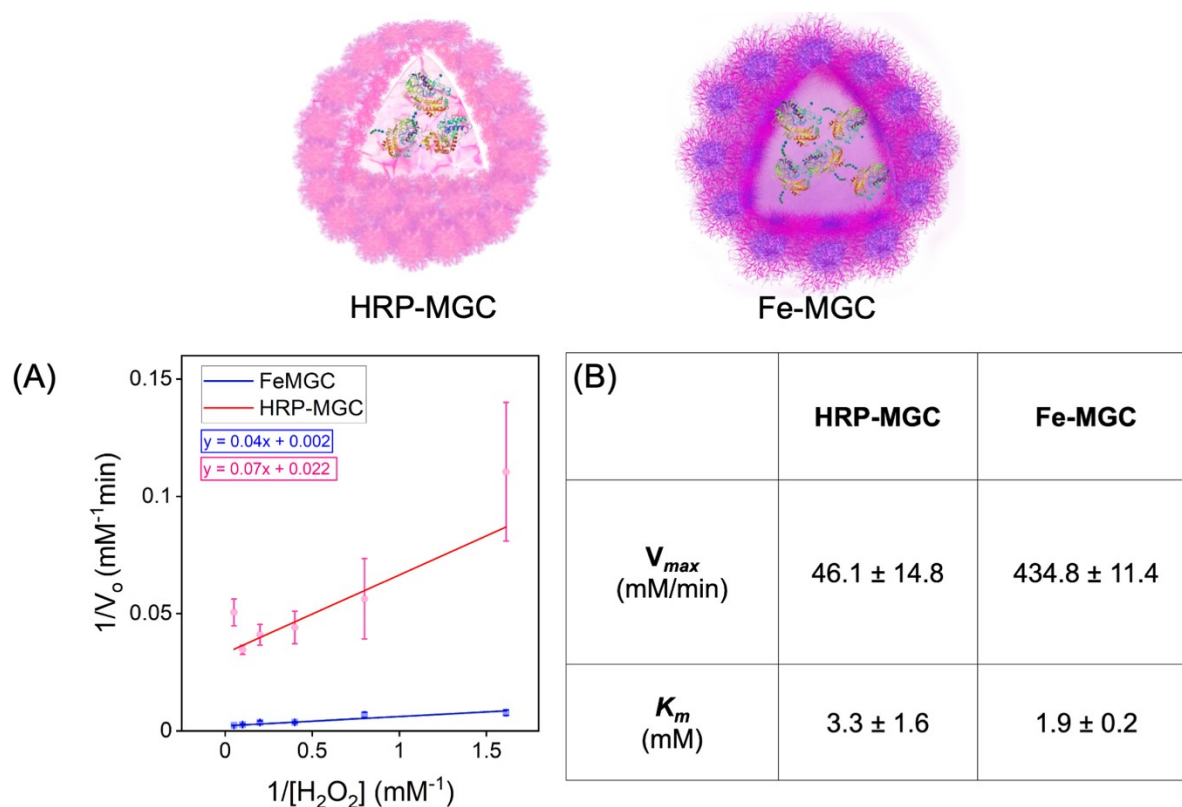


Figure S8. Lineweaver Burk plot and kinetic parameters (V_{max} and K_m) of microreactors HRP-MGC and Fe-MGC. Error bars represent three replicates.

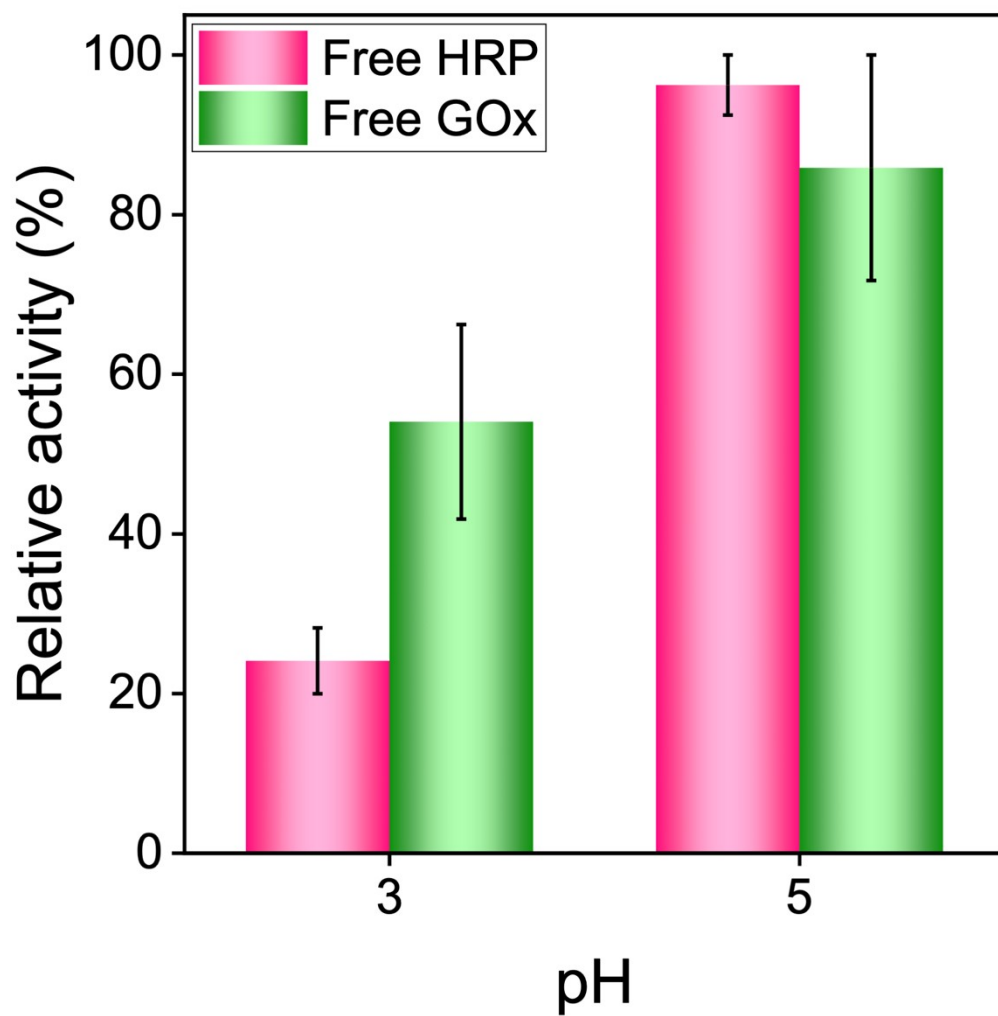


Figure S9. Enzymatic activity of free GOx and HRP at pH 3 and pH 5. Error bars represent three replicates.

Table S1. Encapsulation efficiency of Fe-MGC for different encapsulants.

| Encapsulants | Encapsulation efficiency (%) |
|--------------|------------------------------|
| FITC-dextran | 91.98 ± 3.51 |
| GOx | 95.78 ± 3.30 |
| HRP | 96.69 ± 3.01 |
| GOx-HRP | 94.37 ± 4.46 |

Table S2. Specific activity (V_o) of microgelsomes microreactor for the oxidation reaction at different pH values. Error bars represent three replicates.

| pH | V_o (GOx-HRP MGC) (U/mg) | V_o (GOx-Fe MGC) (U/mg) |
|------|-------------------------------|------------------------------|
| pH 3 | 1086.96 ± 129.12 | 2061.43 ± 241.58 |
| pH 4 | 146.56 ± 74.79 | 828.13 ± 228.13 |
| pH 5 | 104.05 ± 57.17 | 569.33 ± 92.65 |

References:

1. Gaur, D.; Dubey, N. C.; Tripathi, B. P., *Biomacromolecules* **2024**, 25 (2), 1108-1118.
2. Yuan, B.; Chou, H.-L.; Peng, Y.-K., *ACS Applied Materials & Interfaces* **2022**, 14 (20), 22728-22736.